BUBBLE DYNAMICS UNDER AN IMPINGING JET

Ahmed A.B. and Hamed M.S.*
*Author for correspondence
Department of Mechanical Engineering,
McMaster University,
Hamilton, ON,
Canada,
E-mail: hamedm@mcmaster.ca

ABSTRACT

Wall heat flux in the case of jet boiling is greatly dependent on bubble size under the jet. A new force balance model has been proposed to determine bubble size addressing the dynamic effect of the jet on a growing bubble. Jet dynamics cause extra two force components compared to flow boiling case: asymmetric bubble growth force for a moving fluid and pressure force caused by jet stagnation. The model can not be completed without studying bubble growth under the jet. Bubble growth has been studied in the stagnation region for jet velocity of $0.65, 0.8$, and 0.9 m/s and degrees of subcooling of $13, 20$, and 30 °C and in the parallel flow region for jet velocity of 0.85 m/s and 7 °C of subcooling. The instantaneous diameter of the bubble has been measured on the boiling surface by a high speed camera. As the force balance depends on bubble growth rate, Zuber model for non-uniform temperature field is found to best represent the experimental data with different b values.

INTRODUCTION

Boiling is a complex phenomenon and jet dynamics add to its complexity. Several attempts have been made to estimate the wall heat flux under the jet. The common approach for several decades was an empirical approach where the wall heat flux is related to the degree of superheat [1–5]. Recently, studies followed a mechanistic approach in which the wall heat flux is partitioned into different components. Each component represents a physical mechanism of heat transfer on the surface (e.g. forced convection component, evaporation component, and transient conduction component) [6–8].

Omar [8] studied jet impingement subcooled nucleate boiling under steady-state conditions. He developed a partitioning model for jet impingement boiling for jet velocities ranging from 0.4 m/s to 1.7 m/s and degrees of subcooling from 10 to 28°C. The model was developed for impinging jet boiling with no distinction between the parallel flow region and the stagnation region. This was one of the first trails to partition the wall heat flux under an impinging jet. The followed approach was similar to an earlier partitioning model for flow boiling [9]. Heat is being transferred to the superheated liquid layer, as shown in Figure 1, then to the liquid or bubbles on the surface. Omar assumed single phase heat transfer until onset of nucleate boiling (ONB). After ONB, a significant enhancement in single phase component occurs due to the turbulence induced by bubbles attached to the surface. The wall heat flux is partitioned into two components: single phase convection and transient conduction. The wall heat flux can be expressed as,

$$q_w = q_{fc} + q_{tc} \tag{1}$$

where q_{fc} is the forced convection component and q_{tc} is the transient conduction component. Bubble state plays a major role in the magnitude of each component.

Omar and Hamed [10] developed a bubble growth termination scenario model to determine bubble state. They calculated the maximum diameter based on both thermal and dynamic equilibrium independently. The thermal and dynamic effects on a growing bubble were decoupled. Bubbles depart the surface at

NOMENCLATURE

ΔT	[K]	Temperature difference
b	[-]	Constant
Cp	[kJ/kgK]	Specific heat
F	[N]	Force
h_{fg}	[kJ/kg]	Latent heat of evaporation
Ja	[-]	Jakob number
k	[W/mK]	Thermal conductivity
L	[m]	Length
q	[W/m^2]	Heat flux
r	[m]	Bubble radius
t	[s]	time
x/w	[-]	Dimensionless distance from jet center

Special characters

α	[m^2/s]	Thermal diffusivity
ρ	[kg/m^3]	Density
θ	[°]	Camera tilt angle
ϕ	[°]	Angle

Subscripts

σ	Surface tension	h	Hydrodynamic
a	Actual	l	Liquid
b	Buoyancy	m	Measured
cp	Contact pressure	tc	Transient conduction
du	Asymmetric growth	v	Vapor
fc	Forced convection	w	Wall

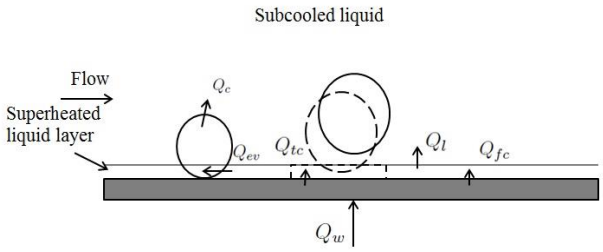

Figure 1. Representation of heat flow path [8]

minimum bubble diameter attained from (i) the thermal equilibrium and (ii) the dynamic equilibrium.

Thermal equilibrium determines the bubble diameter based on balance between the heat flowing to and from the bubble. When the two components equate, the bubble diameter is determined from equilibrium. Dynamic equilibrium determines the bubble diameter based on the balance of forces on the bubble. Omar and Hamed [10] considered drag force, growth force, buoyancy force, and shear lift force. Their model is valid for parallel flow region where the jet is split and the liquid flows parallel to the surface.

Decoupling thermal and dynamic effect is a very idealistic approach for bubble growth under impinging jet. It simplifies the determination of departure diameter by considering each case independently. A more accurate approach is that bubble growth is controlled by thermal equilibrium while departure is controlled by net forces on the bubble. Following is a review of the relevant bubble growth models and a new proposed model for forces on a bubble in the stagnation region of an impinging jet.

BUBBLE GROWTH

Once embryo is formed, bubble growth is characterized by momentum interaction between the growing bubble and the surrounding liquid, i.e. inertia forces. As the bubble grows, heat diffusion between the superheated layer and vapor bubble comes into play till the growth is completely controlled by heat diffusion. The transition between the two growth mechanisms is smooth with no sudden changes in growth rate or size [11]. For example, at low pressure boiling, the growth is mainly controlled by inertia force. While at high pressure, bubble growth predominately controlled by heat diffusion [12].

With advancement in bubble growth time, heat diffusion growth is more significant. Bubble growth depletes energy from the superheated layer resulting in a decrease in the vapor temperature. Hence, the growth rate decreases as bubble growth is controlled by the slow heat diffusion. Plesset and Zwick [13] studied bubble growth in a superheated liquids. They developed a relation for bubble radius in superheated liquid as follows,

$$r = 2\sqrt{3}\, Ja_{sup} \sqrt{\frac{\alpha t}{\pi}} \tag{2}$$

where r is bubble radius, Ja is Jakob number, α is thermal diffusivity, and t is growth time.

Zuber [14] solved the one dimensional, transient heat conduction problem for uniform temperature field and for non-uniform temperature field as the follows,

$$r(t) = b\sqrt{\frac{\alpha t}{\pi}}\,\frac{\Delta T C_p \rho_l}{h_{fg}\,\rho_v}\left[1 - \frac{q_b\sqrt{\pi\alpha t}}{2k\,\Delta T}\right] \tag{3}$$

where b is constant, k is liquid thermal conductivity and q_b is heat flux to the bulk liquid. q_b vanishes when the temperature is uniform around the bubble or when the bubble just departed the nucleation site after reaching its maximum diameter. Then equation 3 is expressed as,

$$r(t) = 2bJa_{sup}\sqrt{\frac{\alpha t}{\pi}} \tag{4}$$

While Zuber model was developed only for diffusion growth, Mikic et al. [12] developed a bubble growth model applicable for the whole range of bubble growth, including both inertial and diffusion growth for uniformly and non-uniformly superheated liquid. Their model, in a non-dimensional form, for non-uniform temperature field can be written as,

$$r^+(t) = t^{+0.5}\left(1 - \theta\left[\left(1 + \frac{t_w^+}{t^+}\right)^{0.5} - \left(\frac{t_w^+}{t^+}\right)^{0.5}\right]\right) \tag{5}$$

$$t^+ = \frac{A^2}{B^2}\,t$$

$$r^+ = \frac{B^2}{A}\,r$$

$$\theta = \frac{T_w - T_l}{\Delta T}$$

Where, A and B are related to the wall superheat as follows,

$$A = \left[b\frac{h_{fg}\,\rho_v\,\Delta T_{sat}}{\rho_l\,T_{sat}}\right]^{1/2} \tag{6}$$

$$B = \left[\frac{12}{\pi}\alpha_l\right]^{1/2} Ja \tag{7}$$

$$Ja = \frac{\Delta T_{sat}\,c_{pl}\,\rho_l}{h_{fg}\,\rho_v} \tag{8}$$

where $b = \pi/7$ for bubble growth on a surface, t_w^+ is a non-dimensional waiting time. Waiting time is often assumed to be equal to the bubble growth time, while the inverse of the sum of both times give the bubble release frequency. Mikic et al. [12] collected waiting time data from the experiments carried out to measure the diameter. They found that for $t^+ \ll 1$, $r \sim t$ (inertial growth) while at $t^+ \gg 1$, $r \sim \sqrt{t}$ (heat diffusion growth).

FORCES ON A GROWING BUBBLE

Bubble growth under impinging jets has different characteristics than the extensively studied pool boiling and flow boiling as the jet hydrodynamics add extra forces on growing bubble in the vertical direction. The proposed forces are based on the forces acting on a bubble in flow boiling [15, 16]. The forces acting on a growing bubble under the jet are shown in Figure 2. The force balance in the y-direction can be expressed as,

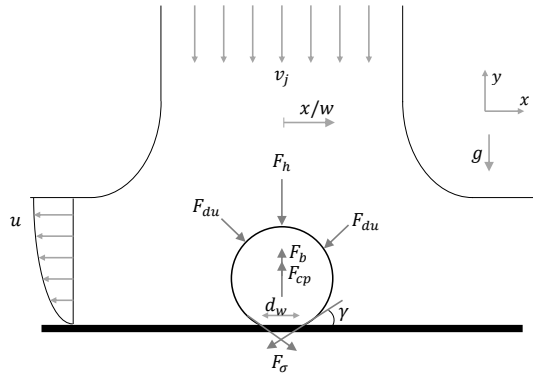

Figure 2. Forces acting on growing bubble in the stagnation region

$$\sum F_y = F_\sigma + F_{du} + F_{cp} + F_b + F_h \tag{9}$$

where, F_σ is y-direction surface tension, F_{du} is asymmetric growth force, F_{cp} is contact pressure force, F_b buoyancy force, and F_h is hydrodynamic pressure force caused by the jet. In the stagnation region, the x-direction forces are balanced and no information may be inferred from it.

It worth noting that force balance requires the instantaneous bubble diameter and the growth rate to accurately calculate each force component.

CURRENT WORK

The current work is an experimental study of bubble growth under an impinging jet in the stagnation region ($x/w \leq \pm 2$) as well as the parallel flow region ($x/w > \pm 2$). The instantaneous diameter of growing bubbles is measured using a series of high speed images at 6000 fps.

Bubbles' diameter is measured in the parallel flow region for jet velocity of 0.85 m/s, 7 °C of subcooling and 10 °C of superheat [17]. As literature is short on stagnation region, bubbles' diameter is measured in the stagnation region at 37 °C of superheat for jet velocities of $0.65, 0.8$, and 0.9 m/s and degrees of subcooling of $13, 20$, and 30 °C.

EXPERIMENTAL SETUP

A copper surface is heated indirectly by three 25 μm-thick NiCr 80/20 foils from the bottom, as shown in Figure 3. The surfaces is cooled by an 8-mm planar water jet. A thin layer of thermally conductive and electrically insulating material, OMEGATHERM 201, is sandwiched between the foils and the copper surface to eliminate short circuit and insure high thermal conductivity. Three DC power supplies are used to supply DC current to the foils. Each power supply is controlled separately to achieve uniform constant temperature. Proportional Integral (PI) LabVIEW controller is used to maintain the same surface temperature over the entire surface regardless of the surface heat flux.

Distilled water is pumped from a thermostatic control heated water tank to the nozzle. After impinging the surface the water is collected back to the tank. The loop is fitted with a turbine flow meter, a thermocouple, and a pressure gauge.

The surface is prepared before each experiment. It is pressed against a fine sandpaper then cleaned with acetone. The surface roughness (Ra) was measured, at two different points on the surface on the surface after two random preparation procedure and it was around 110 nm.

Eighteen 0.5 mm K-type thermocouples are inserted half way through holes in the copper block forming two rows. The holes were filled with thermal oil before inserting the thermocouples. The thermocouples are fixed in position with high temperature epoxy. K-type thermocouples are used because they are known for their minimal thermal drift over long period of time and at high temperatures.

Temperature readings are fed into an inverse heat conduction solver, INTEMP, to estimate the surface temperature and wall heat flux. Temperatures inside the body of the copper block are enough to drive an accurate estimate without the need to account for heat losses from the foil to the ceramic base.

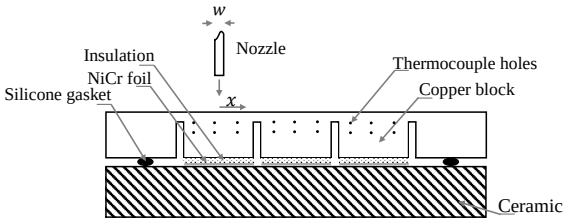

Figure 3. Three module heater test section

HIGH SPEED IMAGING

A high speed camera is set in two positions: (i) parallel to the surface (position (1) in Figure 4), and (ii) tilted with an angle, θ, from the vertical line (position (2) in Figure 4). Position (1) captures real dimensions of the bubble and requires less processing time. However, bubble distinction is hard as many bubbles across the boiling surface are pictured. Bubbles close to the camera hide other bubbles in the middle. Position (2) is more preferable than position (1). Although tilting the camera at the surface requires correcting the measured lengths and angles measured, it widens the frame and allow more bubbles to be pictured without overlapping. By setting a scale onto the surface, vertical dimensions

measured could be corrected as follows,

$$L_a = L_m \cos\theta \tag{10}$$

$$\phi_a = \tan^{-1}\frac{\tan\phi_m}{\cos\theta} \tag{11}$$

where L_a is the actual length, L_m is the measured length, θ is the camera tilt angle, ϕ_a is the actual angle, and ϕ_m is the measured angle.

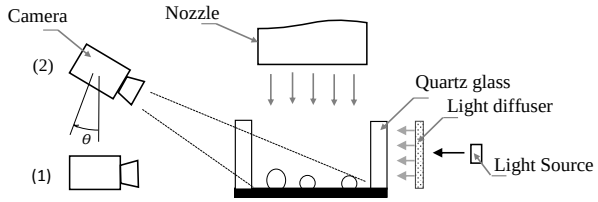

Figure 4. Tilted lengths and angles

EXPERIMENTAL RESULTS

Bubbles are present on the surface since their incipience at ONB. Bubbles' frequency and active nucleation sites increase with the degree of wall superheat increase until fully developed nucleate boiling where bubbles cover the whole surface. Bubble growth is vital for estimation of forces acting on a bubble and for wall heat flux calculations. Calculations of the forces are dependent on the instantaneous bubble diameter and its rate of change. Bubbles' diameter is measured from incipience to lift-off. As the high speed camera is set to 6000 fps, the step in time is the multiples of $1/6$ ms. Bubbles' diameter was measured and tracked at each time step of bubbles' life.

Stagnation Region

As Thermal Boundary Layer (TBL) is thinner in the case of impingement jet than flow boiling or pool boiling, bubble diameter is bigger than the TBL causing condensation at the top cap of the bubble. Condensation is balanced with evaporation caused by the superheated layer. The result is smaller bubble diameter. Bubble does not depart until the point at which the vertical forces on the bubble act to detach it from the surface ($\Sigma F_y \neq 0$).

As the bubble growth is controlled by thermal diffusion, Zuber model (equation 3) can represent bubble growth. The value of b constant is found to be $\pi/7$. The model estimated the mean bubble diameter in the stagnation region for different conditions of jet velocities ($0.65, 0.8$ and 0.9 m/s) and degrees of subcooling ($13, 20$ and 30 °C). All the experiments were carried out at 37 °C of superheat. Zuber's model showed good agreement with the experimental measured data except at low jet velocities and high degrees of subcooling where the bubble diameter decrease before it lift-off or completely collapse. The estimated bubble diameters for two cases are shown in Figure 5 and Figure 6.

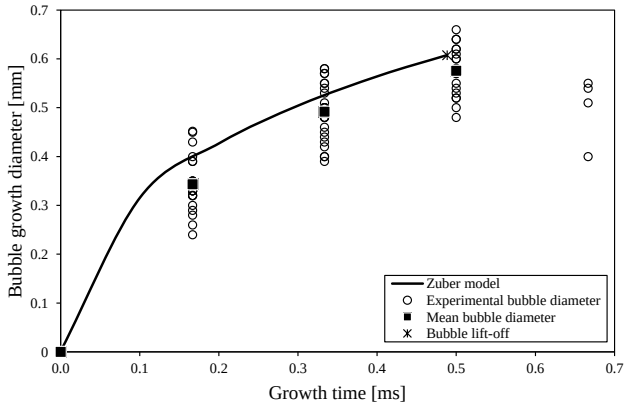

Figure 5. Experimental bubble diameter and Zuber model for jet velocity of 0.8 m/s and 20 °C of subcooling

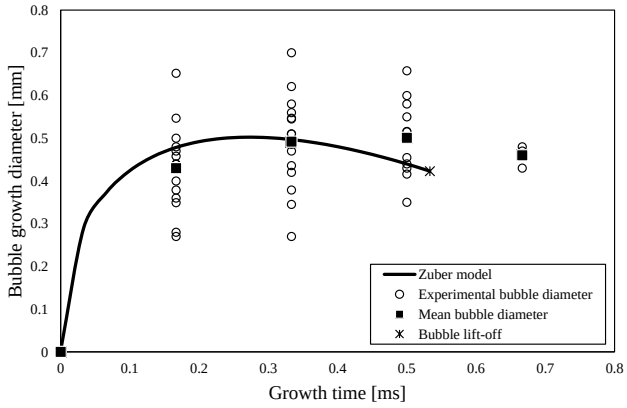

Figure 6. Experimental bubble diameter and Zuber model for jet velocity of 0.65 m/s and 13 °C of subcooling

The estimated bubble growth diameter is compared to the experimental measurements and to the mean diameter, as shown in Figure 7. The model has normalized root mean square error (NRMSE) of 21% for the mean diameter and 25% for all the experimental data.

Parallel Flow Region

The boiling surface in the parallel flow region was pictured under water jet velocity of 0.85 m/s, 7 °C of subcooling and 10 °C of superheat. The bubble diameter was observed to increase with the distance from the jet. For example, the most probable bubble diameters for nucleation sites $x/w = 16$ is 0.8 mm compared to 2.1 mm for $x/w = 22$. The previous observation coincide with the current understanding of the jet dynamics. The jet cause a thin boundary layer and hence smaller bubbles [18]. Also the degree of superheat required to start bubble growth is decreased with the distance from the jet, as shown in Figure 8. This is because of the growth of the TBL over the parallel flow region.

Mikic et al. [12] model, equation 5, was initially used to estimate the bubble growth diameter for bubbles away from the

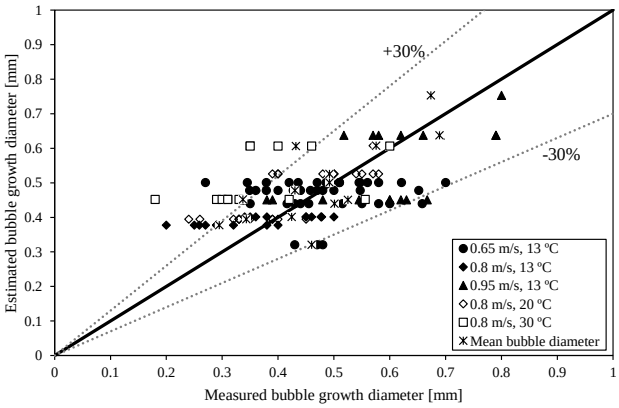

Figure 7. Experimental bubble diameter vs estimated bubble diameter in the stagnation region

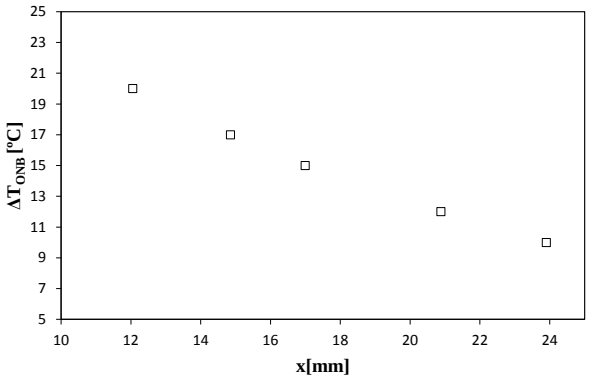

Figure 8. Location of the first bubble on the surface [17]

jet. Their proposed relation is considered as the average between the linear growth in the inertia controlled growth and the power growth in the heat diffusion controlled growth. The model fits the data reasonably, but it does not predict the reduction in diameter due to the condensation close to lift-off. Figure 9 shows Mikic model against experimental data for different waiting times. The waiting time data were collected for the average time taken between first bubble departure and successive bubble incipience from the same nucleation site. On the other hand, Zuber's model, as shown in Figure 9, showed better agreement with the experimental data and counted for the condensation at the top of the bubble. The different values for, q_b are obtained from solving the inverse heat conduction problem and estimating the heat flux at different values of x/w. Comparison between the experimental data and the estimated values of bubble diameter for different values of x/w is shown in Figure 10. The model tends to overestimate the growth rate for $x/w = 16$ and 22. The model has a normalized root mean square error (NRMSE) of 31% for the parallel flow region.

CONCLUSIONS

Mechanistic modeling of the wall heat flux is a complex process that requires deep understanding of the underlying physics.

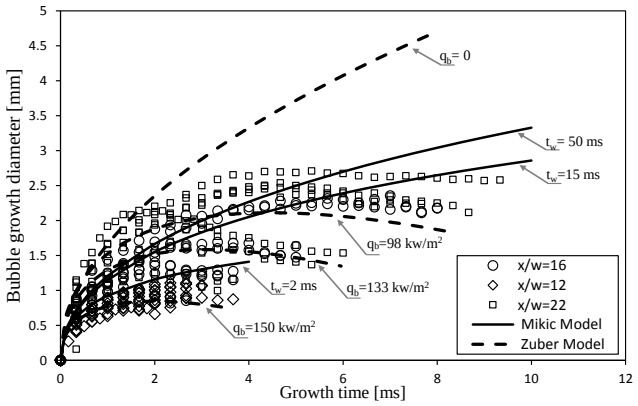

Figure 9. Bubble growth diameter for 0.85 m/s jet velocity and 7 °C of subcooling compared to Zuber and Mikic model

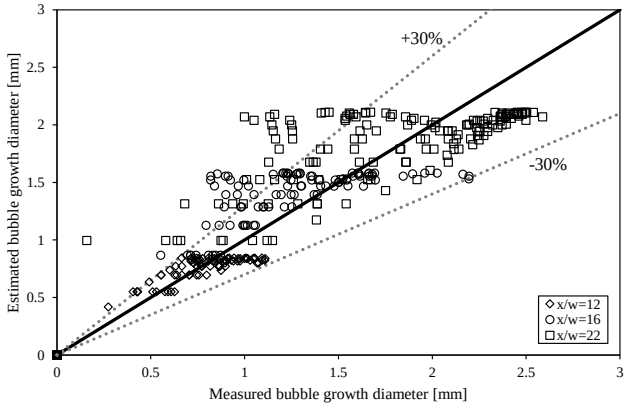

Figure 10. Estimated values of Zuber model vs experimental data for parallel flow region

Bubble growth modeling is the base stone in understanding the forces on a growing bubble and hence wall heat flux. Thermal Processing Laboratory (TPL) is studying impingement jet boiling for over a decade now. The current work is under continuous improvement to introduce a sound wall heat flux mechanistic model. Bubble growth is modeled for both stagnation and parallel flow regions. Zuber model is found to best describe the bubble growth with different b values; $\pi/7$ and $5\pi/6$ for stagnation and parallel flow regions respectively. A new force model is being developed for the stagnation region.

ACKNOWLEDGMENT

The authors would like to acknowledge the financial support received from the Natural Sciences and Engineering Research Council of Canada (NSERC).

REFERENCES

[1] Ishigai, S., Nakanishi, S., and Ochi, T., Boiling heat transfer for a plane water jet impinging on a hot surface, in *Sixth International Heat Transfer Conference*, Toronto, ON, Canada, pp. 445–4450.

[2] Miyasaka, Y., Inada, S., and Owase, Y., Critical heat flux and subcooled nucleate boiling in transient region between a two-

dimensional water jet and a heated surface., *Journal of Chemical Engineering of Japan*, 1980, Vol. 13, No. 1, pp. 29–35.

[3] Katto, Y. and Kunihiro, M., Study of the mechanism of burn-out in boiling system of high burn-out heat flux, *Bulletin of JSME*, 1973, Vol. 16, No. 99, pp. 1357–1366.

[4] Ma, C.F. and Bergles, A.E., Jet impingement nucleate boiling, *Int. J. Heat Mass Transfer*, 1986, Vol. 29, No. 8, pp. 1095–1101.

[5] Hall, D.E., Incropera, F.P., and Viskanta, R., Jet impingement boiling from a circular free-surface jet during quenching: Part 1-Single-phase iet, *Journal of Heat Transfer*, 2001, Vol. 123, No. 5, p. 901.

[6] Ahmed, A.B. and Hamed, M.S., Experimental Investigation of Boiling Under a Planar Water Jet, in *9th International Conference on Boiling and Condensation Heat Transfer, Apr 26-29*, Boulder, CO.

[7] Ahmed, A. and Hamed, M., Modeling of transition boiling under an impinging water jet, *International Journal of Heat and Mass Transfer*, 2015, Vol. 91, pp. 1273–1282.

[8] Omar, A., *Experimental study and modeling of nucleate boiling during free planar liquid jet impingement*, Ph.D. thesis, McMaster University, 2010.

[9] Basu, N., Warrier, G.R., and Dhir, V.K., Wall Heat Flux Partitioning During Subcooled Flow Boiling: Part 1Model Development, *Journal of Heat Transfer*, 2005, Vol. 127, No. 2, pp. 131 – 140.

[10] Omar, A. and Hamed, M.S., Modeling of bubble growth under an impinging free planar water jet, *ASME Journal of Heat Transfer Engineering*, 2016, Vol. 37, No. 18.

[11] Robinson, a.J. and Judd, R.L., The dynamics of spherical bubble growth, *International Journal of Heat and Mass Transfer*, 2004, Vol. 47, No. 23, pp. 5101–5113.

[12] Mikic, B., Rohsenow, W., and Griffith, P., On bubble growth rates, *International Journal of Heat and Mass Transfer*, 1970, pp. 657–666.

[13] Plesset, M.S. and Zwick, S.a., The growth of vapor bubbles in superheated liquids, *Journal of Applied Physics*, 1954, Vol. 25, No. 4, pp. 493–500.

[14] Zuber, N., *Hydrodynamic aspects of boiling heat transfer*, Ph.D. thesis, 1959.

[15] Klausner, J., Mei, R., Bernhard, D., and Zeng, L., Vapor bubble departure in forced convection boiling, *International Journal of Heat and Mass Transfer*, 1993, Vol. 36, No. 3, pp. 651–662.

[16] Zeng, L., Klausner, J., Bernhard, D., and Mei, R., A unified model for the prediction of bubble detachment diameters in boiling systems II. Flow boiling, *International Journal of Heat and Mass Transfer*, 1993, Vol. 36, No. 9, pp. 2271–2279.

[17] Ahmed, A.B. and Hamed, M.S., Bubble dynamics under an impinging planar water jet, in *10th International Conference of Heat Transfer, Fluid Mechanics and Thermodynamics, 14 - 16 July - HEFAT2014*, Orlando, FL.

[18] Wolf, D. and Incropera, F., Jet impingement boiling, *Advances in Heat Transfer*, 1993, Vol. 23, pp. 1–132.